Journal of Engineering Science and Technology
Vol. 7, No. 3 (2012) 303 - 321

PERFORMANCE ANALYSIS OF OPTICAL CDMA SYSTEM USING VC CODE FAMILY UNDER VARIOUS OPTICAL PARAMETERS

HASSAN YOUSIF AHMED[1,*], M. ALMALEEH[2], HILAL FADHIL[3], S. A. ALJUNID[3], AMMAR E. BABIKER[4], N . M. SAAD[4]

[1]Electrical & Electronic Engineering Department, Faculty of Engineering, Salman bin Abdulaziz University, Wadi Aldoassir, Kingdom of Saudi Arabia
[2]Faculty of Engineering, Electronics Engineering Dept, University of Gezira, Sudan
[3]School of Computer and Communication Engineering, Universiti Malaysia Perlies, Malaysia
[4]Electrical & Electronic Engineering Department, Universiti Teknologi Petronas, Bandar Seri Iskandar, 31750 Tronoh, Perak, Malaysia
*Corresponding Author: hassanuofg@gmail.com

Abstract

The intent of this paper is to study the performance of spectral-amplitude coding optical code-division multiple-access (OCDMA) systems using Vector Combinatorial (VC) code under various optical parameters. This code can be constructed by an algebraic way based on Euclidian vectors for any positive integer number. One of the important properties of this code is that the maximum cross-correlation is always one which means that multi-user interference (MUI) and phase induced intensity noise are reduced. Transmitter and receiver structures based on unchirped fiber Bragg grating (FBGs) using VC code and taking into account effects of the intensity, shot and thermal noise sources is demonstrated. The impact of the fiber distance effects on bit error rate (BER) is reported using a commercial optical systems simulator, virtual photonic instrument, VPITM. The VC code is compared mathematically with reported codes which use similar techniques. We analyzed and characterized the fiber link, received power, BER and channel spacing. The performance and optimization of VC code in SAC-OCDMA system is reported. By comparing the theoretical and simulation results taken from VPITM, we have demonstrated that, for a high number of users, even if data rate is higher, the effective power source is adequate when the VC is used. Also it is found that as the channel spacing width goes from very narrow to wider, the BER decreases, best performance occurs at a spacing bandwidth between 0.8 and 1 nm. We have shown that the SAC system utilizing VC code significantly improves the performance compared with the reported codes.

Keywords: Vectors combinatorial (VC), MUI, SAC-OCDMA, BER, FBG.

Nomenclatures

B	Noise-equivalent electrical bandwidth of the receiver, Hz
d_N	Data bit of the Nth user
e	Electron's charge, Coulomb
h	Planck's constant
I	Average photocurrent, A
I^2	Power spectral density for I, W
I_{piin}^2	Phase induced intensity noise (PIIN), W
I_{Tot}^2	Total noise power, W
I_{th}^2	Thermal noise, W/Hz
I_{sh}	Shot noise, W
K_B	Boltzmann's constant
L	VC code length
N	Number of the active users
P	Number of mapping users
P_{sr}	Effective power of a broadband source at the receiver, dBm
R	Number of the remaining users after modulo operation
R_L	Receiver load resistor, Ω
T_n	Absolute receiver noise temperature, K
$u(v)$	Unit step function
V	Column vector
V_c	Central frequency of the original broad-band optical pulse, Hz
v_i	A vector
W	Code weight

Greek Symbols

ΔV	Optical source bandwidth, Hz
η	Quantum efficiency
$\Re$	photodiode responsivity

1. Introduction

Reliable networks with higher throughput, low cost and different classes of services are required. The tremendous growth of the Internet has brought more users online and thus consuming larger amounts of bandwidth. To realize the demands for bandwidth and new services, a new technology must be deployed and fiber optics is one such key technology. Optical fiber offers several advantages over conventional media (e.g., coaxial cable and twisted pair). Recently Optical Code Division Multiple Access (OCDMA) has been proposed as an alternative to frequency- and time-based multiple and multiplexing methods for next generation high speed optical fiber networks [1-4]. The SAC-OCDMA systems have gained more attention since the MUI can be completely eliminated by spectral coding. Many codes appeared in the literature aiming to support optical networks with large numbers of users at different data rates [5-10]. However, some of these codes have much poorer cross correlation (e.g.,

Hadamard code [5]), or the number of available codes is quite restricted (e.g. integer lattice exists for m and k where m and k need to be a co-prime (it is enough if one is an even and the other is odd) [6], a prime number for modified quadratic congruence (MQC) [7], a prime power for modified frequency hopping (MFH) [8], an even natural numbers for modified double code (MDW) [9], and an odd natural numbers for enhanced double weight (EDW) [10,11]. The performance of OCDMA is limited by strong noise originated from other users trying to use the medium simultaneously, referred to as Multi-user Interference (MUI). In order to combat the MUI a proper detection scheme must be applied. Although MUI can be cancelled by a balanced detection scheme, inherent problems of noise still remain labelled as phase induced intensity noise (PIIN) arising from the spontaneous emission from the broadband source.

Therefore, the distance was expected to influence the performance in two means; loss and dispersion. At low transmission rates, the dispersion effect is not significant, the loss would be dominant. Longer fiber optics provides a huge dispersion and attenuation [9]; thus the bit error rate increases. In particular, the relationship between BER and data rate is inversely proportional, which means as the date rate increased, the BER becomes worse and vice versa. In this paper, we have reviewed an efficient method to construct a new code family and its properties for the SAC-OCDMA systems. This new code family not only possesses ideal in-phase cross correlation, but also exists for a much wider number of the weights for any users while the number of users is greater than the weight plus one is satisfied regardless whether the number is even, odd, prime, prime power, etc. We have proposed a new vector combinatorial (VC) code family for the SAC-OCDMA systems that is characterized by (L, N, W, λ) with length L, number of users N, weight W (number of marks) and cross correlation (CC) λ. In recent years, FBGs have emerged as an enabling technology for many light wave communications. Therefore, FBGs are more convenient for SAC-OCDMA code applications [12].

The complementary detection scheme can be used to give accurate results when the CC is fixed [5]. However, in order to increase the number of users for a VC, a mapping technique must be applied. The mapping technique is a mechanism used in [9, 13] in order to increase the number of users beyond the basic number of users offered by the basic matrix for a specific weight. When applying the mapping technique, the cross CC is no longer fixed, consequently, the complementary detection technique cannot be used to give accurate results. The detection technique proposed in [14] can be used even though the CC between different users is not fixed. A novel encoder/decoder based on FBGs has been proposed in [14]. Similarly we have designed the encoder-decoder structure based on our new proposed codes. We have also analyzed the system by Gaussian approximation taking into account the effects of PIIN, thermal noise and shot noise. The rest of this paper is organized as follows. The family of newly constructed codes is described in Section 2. Section 3 demonstrates the transmitter and receiver structure. Section 4 presents the analytic results of system performance. The property of this code is discussed from the view of comparison in Section 5. Theoretical analysis and simulation results are drawn in Section 6. Finally, we have the conclusion in Section 7.

2. The VC Code Construction and Properties

Definition: In mathematics, the standard basis of the *W*-dimensional Euclidean space R^W is the basis obtained by taking the *W* (code weight) basis vectors [15]:

$\{v_i: 1 \le i \le W\}$

where v_i is the vector with a 1 in the *ith* coordinate and 0 elsewhere.

For example, the standard basis for R^4 (i.e., *W*=4) is given by the five vectors as:

$$\boldsymbol{v}_1 = \begin{pmatrix} 1 \\ 0 \\ 0 \\ 0 \end{pmatrix} \quad \boldsymbol{v}_2 = \begin{pmatrix} 0 \\ 1 \\ 0 \\ 0 \end{pmatrix} \quad \boldsymbol{v}_3 = \begin{pmatrix} 0 \\ 0 \\ 1 \\ 0 \end{pmatrix} \quad \boldsymbol{v}_4 = \begin{pmatrix} 0 \\ 0 \\ 0 \\ 1 \end{pmatrix} \tag{1}$$

The design of new proposed code family which is referred to as vector combinatorial (VC) code, can be constructed by dividing the code construction into three steps which are vector construction, vectors combination and mapping technique.

Step 1, Vector construction: based on the standard basis, we first construct a column vector having only two "1" which will make the cross-correlation exactly equal to 1. Let $V_{(i, i+1)}$ be a column vector whose *ith* element is one and others are zeros and its length equals *N* as follows.

$$V_{(i,\,i+1)} = \begin{pmatrix} 1 \\ 0 \\ . \\ . \\ 1 \end{pmatrix} \tag{2}$$

Step 2, Vectors combination: in order to make the in-phase CC exactly equal to 1 in each column while maintaining the weight value in the row (code word for each user), every vector in the matrix (see Fig. 1) is indexed as $V_{(i, i+1)}$ for *i* fixed to user arrangement and *i*+1 shifts to the down by one up to *N* to make the CC with *N*-1 is exactly equal to 1 (i.e., for *N*=5 (vector length), the maximum value of *i*= *N*-1 which is 5-1=4. Therefore for *N*=4, the columns vectors corresponding *i* values will be calculated as: *i*=1; $V_{(i, i+1)}= V_{12}, V_{13}, V_{14}$; for *i*=2, $V_{(i, i+1)} = V_{23}, V_{34}$; for *i*=3, $V_{(i, i+1)}=V_{34}$ which means *i* represents number of row (user). In Fig. 1, we have shown the procedure of generating (0,1) sequence after combining all columns vectors. To be more precise from the figure we can observe that each column vector contains two "1"s; *W* represents number of "1"s per row; *N* are number of rows (number of users).

Thus, the sequence $(V_{12}V_{13}...V_{1N})(V_{23}V_{24}...V_{2N})....(V_{(N-1)N}$ gives a code having ideal in-phase CC (λ=1) called ideal case (IC).

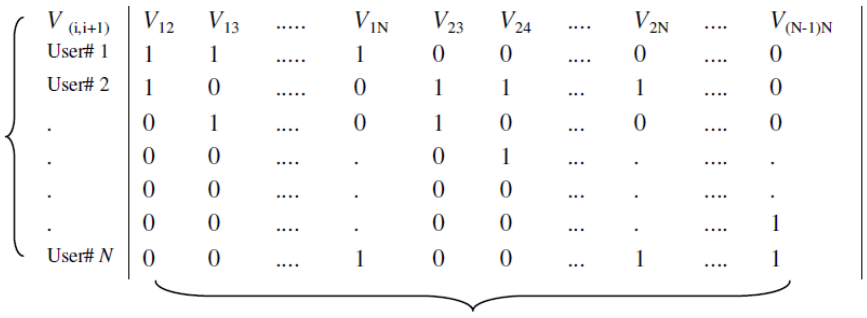

$V_{(i,i+1)}$	V_{12}	V_{13}	.....	V_{1N}	V_{23}	V_{24}	....	V_{2N}	....	$V_{(N-1)N}$
User# 1	1	1	.....	1	0	0	....	0	....	0
User# 2	1	0	.....	0	1	1	...	1	....	0
.	0	1	....	0	1	0	...	0	....	0
.	0	0	....	.	0	1	...	.	....	.
.	0	0	....	.	0	0	...	.	....	.
.	0	0	....	.	0	0	...	.	....	1
User# N	0	0	....	1	0	0	...	1	....	1

Fig. 1. A General Matrix of VC when $N=W+1$.

Step 3, Mapping technique:

Although the IC can be constructed easily using a column vector, the requirement that N-1=W must be satisfied limits the number of users. To overcome this problem, a mapping technique must be applied (see Fig. 2). The mapping technique is a mechanism used in [9, 13] in order to increase the number of users beyond the basic number of users offered by the basic matrix for a specific weight. Therefore, N can be written as follows

$$N=P(W+1)+R \tag{3}$$

where P, R are positive integer numbers represent number of (W+1) repeating in diagonal fashion, and the remaining users after module division for N respectively, and R can be expressed as:

$$R=N \bmod P(W+1) \tag{4}$$

To clarify steps (2) and (3) where *mod* represents modulo division, let us consider the example N=8, W=2, substitute the values in (2), gives 8=2× (2+1) +2, which means P=2 and R=2. For N=9, W=2, gives 9=3×(2+1)+0 which means P=3 and R=0.

In order to increase the number of users in VC code family, a mapping technique must be applied. The mapping technique (see Fig. 2) operates by diagonally repeating the IC for the (W+1) users P-times and filling the empty spaces with zeros.

The length of that part is $P.\frac{W(W+1)}{2}$. Consequently, an IC with the parameters (W, R) must be added if $R<W+1$ is satisfied (i.e., $R=N \bmod P$ (W+1) ≠0) (see Fig. 2). The length of that second part of the code is $\frac{R\times(2W-R+1)}{2}$. Finally, the whole length L is given by:

$$L=\frac{PW(W+1)}{2}+\frac{R(2W-R+1)}{2}=\frac{WN+R(W+1-R)}{2} \tag{5}$$

In Table 1, W = 3 and N = 9 by using (4), (5) gives 9=2× (3+1) +1, resulting P=2 and R=1 which means we have to repeat the IC two times (P=2) in diagonal fashion resulting in 8 users and add one more user (R=1) after user#8 in diagonal fashion as well. By using (6) L= 9×3+1(3-1+1)/2, the length will be 15. In Table 1, there are three groups, the first group of the code (the first six columns) is the VCC with the parameters (3,4) which means W=3 and N=4 having a CC equal to 1, the second group (the columns from 7 to 12) is a replica from the first group with the parameters (3, 4), the third group (the columns 13, 14, 15) is the VCC with the parameters (3,1) which means W=3 and N=1(i.e., R=N) since the condition $R<W+1$ (1<4) is satisfied having a CC equal to 1.

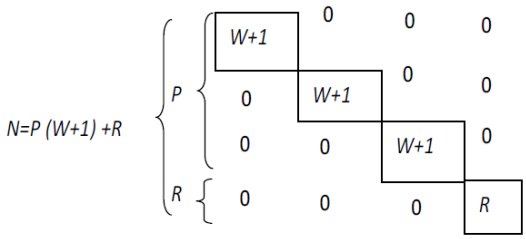

Fig. 2. A Graphic Representation of Mapping Techniques for N= P (W+1)+R.

Table 1. VC Code for $N > W$+1(N=9, W=3)

P=2	W+1=4	1	1	1	0	0	0	0	0	0	0	0	0	0	0
		1	0	0	1	1	0	0	0	0	0	0	0	0	0
		0	1	0	1	0	1	0	0	0	0	0	0	0	0
		0	0	1	0	1	1	0	0	0	0	0	0	0	0
	W+1=4	0	0	0	0	0	0	1	1	1	0	0	0	0	0
		0	0	0	0	0	0	1	0	0	1	1	0	0	0
		0	0	0	0	0	0	0	1	0	1	0	1	0	0
		0	0	0	0	0	0	0	0	1	0	1	1	0	0
	R=1	0	0	0	0	0	0	0	0	0	0	0	0	1	1	1

3. Structure of Transmitter and Receiver

3.1. Structure of transmitter and receiver based on FBG

As shown in Table 1, the VC code words of 9 users are obtained by applying the mapping technique. Figure 3 represents the corresponding amplitude spectra of the code sequences, where the solid lines represent one chip and the dash lines represent zero chips.

In the VC family, the code construction depends on the number of users, so if the number of users N is greater than the weight plus one *(N>W+1),* a mapping technique must be applied resulting in the CC no longer being fixed. A Hybrid Wavelength-Division-Multiplexing/Spectral-Amplitude-Coding Optical CDMA System (WDM/SAC) is proposed in [14], where balance detection can be achieved even though the CC value is not fixed.

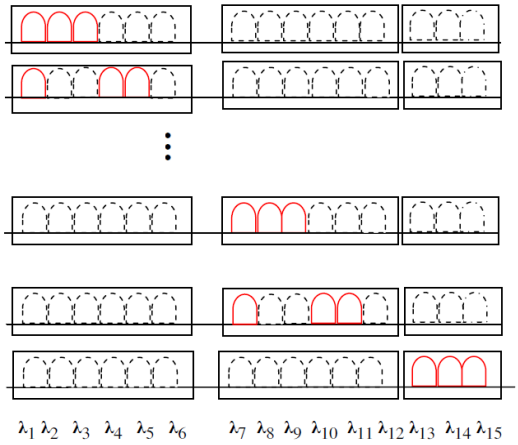

Fig. 3. Spectral of WS-VC Code for 9 Users.

In Fig. 4, similarly we have used the method given in [14] to design the transmitter and receiver structure based on user#1 (111000000000000). ON-OFF shift keying modulation is used to modulate the information bits for the desired user and then the result of the optical signal is directed to FBGs, where each chip of the VC has been attributed by a specific wavelength (λ_1 λ_2 λ_3). The decoding process is similar to conventional SAC systems, and could be achieved by passing the receiving signal through two FBG arrays assigned by the weight (λ_1 λ_2 λ_3) and its complementary (λ_4 λ_5 λ_6) , then recover the signal differentially to reproduce the desired signal [14]. Note that only codes that correlate with intended receiver are circulated to both photo-detectors. Codes that do not correlate pass without getting detected.

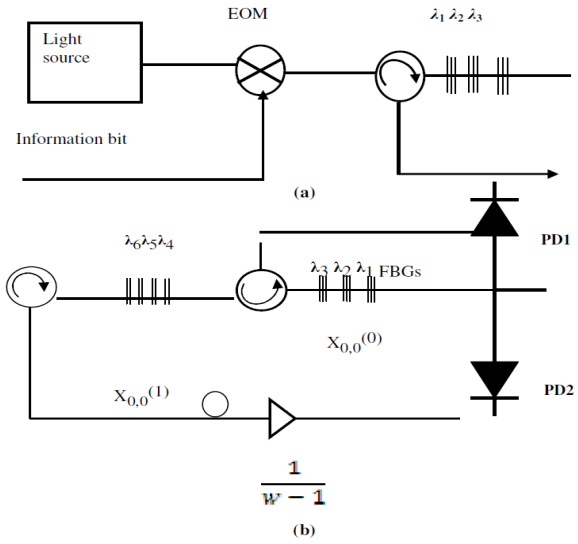

Fig. 4. Structure of (a) Encoder and (b) Decoder for User # 1using VC with Mapping Using FBGs.

3.2. Structure of transmitter and receiver based on VPI

A simple schematic block diagram consists of two users (W=4) as illustrated in Fig. 5 using the simulation software, *Virtual Photonic Instrument* (VPI^{TM}) version 7.1. Each chip has a spectral width of 0.8 nm (100 GHz). The tests were carried out at a data rate of 10 Gb/s for a different distance with the ITU-T G.652 standard single mode fiber (SMF). All the attenuation α (i.e., 16 ps/nm km) and nonlinear effects such as four-wave mixing, the cross phase modulation, and the group delay were activated and specified according to the typical industry values to simulate the real environment as close as possible. At transmitter side, we have a pseudo random bit sequence (PRBS) generator as the input data of each user followed by a coder jitter to generate an NRZ sample ended by a rise time to adjust the rise time of the pulse. After that a Mach-Zehnder modulator is used to modulate the laser output. As shown in Fig. 5 after the splitter, we used a fiber Bragg grating (FBGs) spectral amplitude decoder operates to decode the coded sequence. After that we used a clock recovery ideal to synchronize incoming optical signal with original transmitted signal. The decoded signal was decoded by a photo-detector (PD) followed by a 0.7 GHz low pass filter (LPF) and error detector, respectively. The transmitted power used was 0 dBm of the broadband source. The noise generated at the receiver was set to be random and totally uncorrelated. The dark current value was 5 nA and the thermal noise coefficient was 2.5×e^{-23} W/Hz for each of the photo-detectors.

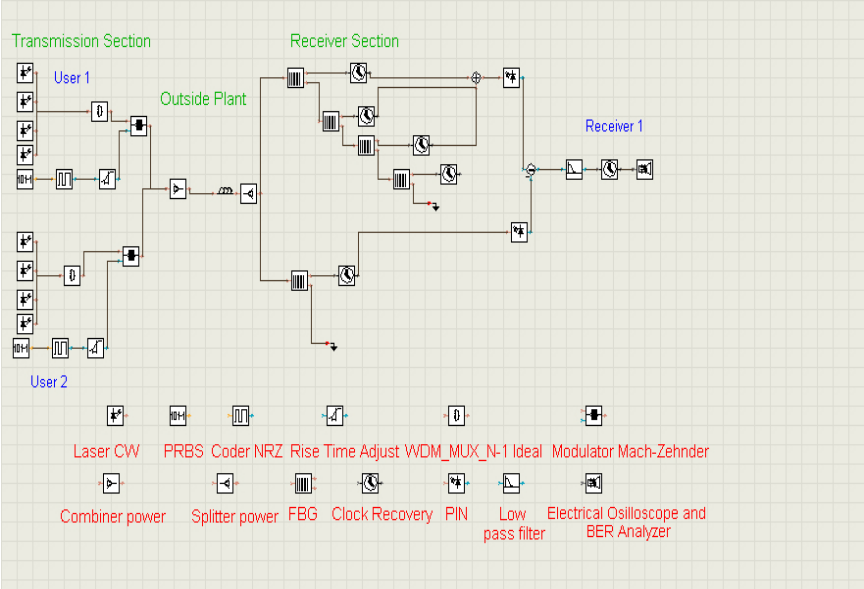

Fig. 5. Simulation Setup of the Proposed VC Code Using a Hybrid WDM/SAC Detection Technique.

4. System Performance Analysis

In our analysis of the proposed system we have considered simultaneously intensity noise (I_{piin}), shot noise (I_{sh}) and thermal noise (I_{th}) in photodiode. The detection scheme for the proposed system is based on a hybrid detection using

optical filter followed by photo-detector. Gaussian approximation is used for the calculation of BER as in [7, 8, 16]. The SNR is calculated at the receiver side and for each user there is only one photodiode, the current flow through the photodiode is denoted by *I*.

Let $C_N(i)$ denote the ith element of the Nth VC code sequence. Assume user# (f, g) is the desired user belong to the ideal case ($N=W+1$) and user# (z, t) does not belong to ideal case ($N=P(W+1)+R$), the correlation functions of each user is given by:

$$PD_1^{(0)}(f,g,z,t)=\begin{cases} W, & f=z \\ 1, & f\neq z, \quad g=t, \ \text{for}\, N=(W+1) \\ 0, & g\neq t, \quad \text{for}\, N=P(W+1)+R \end{cases} \tag{6}$$

and

$$PD_1^{(1)}(f,g,z,t)=\begin{cases} 0, & f=z \qquad\quad g=t \\ W-1, & f\neq z, \quad g=t, \ \text{for}\, N=(W+1) \\ 0, & g\neq t, \quad \text{for}\, N=P(W+1)+R \end{cases} \tag{7}$$

Thus

$$PD_1(f,g,z,t)-\frac{PD_2(f,g,z,t)}{W-1}=\begin{cases} W, & f=z, g=t \\ 0, & \text{else} \end{cases} \tag{8}$$

When a broad-band pulse is input into the group of FBGs, the incoherent light fields are mixed and incident upon a photo-detector, the phase noise of the fields causes an intensity noise term in the photo-detector output. The coherence time of a thermal source (τ_c) is given by [8]:

$$\tau_C=\frac{\int_0^\infty G^2(v)\,dv}{\left[\int_0^\infty G(v)\,dv\right]^2} \tag{9}$$

Where $G(v)$ is the single sideband power spectral density (PSD) of the source. The Q-factor performance provides a qualitative description of the optical receiver performance, the performance of an optical receiver depends on the signal-to-noise ratio (SNR). The Q-factor proposes the minimum SNR required to obtain a specific BER for a given signal. The SNR of an electrical signal is defined as the average signal power to noise power [SNR = I^2/I^2_{Tot}], where I^2_{Tot} is defined as the variance of the noise source (note: the effect of the receiver's dark current and amplification noises are neglected in the analysis of the proposed system), given by

$$I^2_{Tot} = I_{piin} + I_{sh} + I_{th}$$

which also can be written as:

$$I^2_{Tot} = 2eIB + I^2B\tau c + 4K_B\, T_n B R_L \tag{10}$$

In Eq. (10), the first term results from the shot noise, the second term denotes the effect of Phase Intensity Induced Noise (PIIN) [7-10], and the third term represents the effect of thermal noise. The total effect of PIIN and shot noise obeys negative binomial distribution [16]. To analyze the system with transmitter and receiver, we used the same assumptions that were used in [7–10] and are important for mathematical simplicity. Without these assumptions, it is difficult to analyze the system. Assumptions are

- Each light source is ideally unpolarized and its spectrum is flat over the bandwidth [ν_o-$\Delta\nu$/2, ν_o+$\Delta\nu$/2] where ν_o is the central optical frequency and $\Delta\nu$ is the optical source bandwidth in Hertz.
- Each power spectral component has identical spectral width.
- Each user has equal power at the receiver.
- Each bit stream from each user is synchronized.

The above assumption is important for mathematical simplicity. Based on the above assumptions, we can easily analyze the system performance using Gaussian approximation. The power spectral density of the received optical signals can be written as [8]:

$$r(v) = \frac{P_{sr}}{\Delta V}\sum_{N=1}^{N} d_N \sum_{i=1}^{L} c_N(i)\left\{\begin{matrix} u\left[v - v_o - \frac{\Delta v}{2L}(-L+2i-2)\right] \\ -u\left[v - v_o - \frac{\Delta v}{2L}(-L+2i)\right] \end{matrix}\right\} \tag{11}$$

Here the unit step function, $u(v)$, is expressed as:

$$u(v) = \begin{cases} 1, & v \geq 0 \\ 0, & v < 0 \end{cases} \tag{12}$$

Taking into consideration, the effects of shot and thermal noises as well as PIIN have to be analysed. From Eq. (7), the power spectral density at photodetector 1 and photodectotor 2 of the nth (f, g) receiver during one bit period can be written as:-

$$G_1(V) = \frac{P_{sr}}{\Delta V}\sum_{N=1}^{N} d_N \sum_{i=1}^{L} C_N(i)\overline{C}_{(f,g)}(i)\left\{ u\left[V - V_0 - \frac{\Delta V}{2L}(-L+2i-2)\right] \right. \tag{13}$$

$$\left. - u\left[V - V_0 - \frac{\Delta V}{2L}(-L+2i)\right] \right\}$$

$$G2(V) = \frac{P_{sr}}{\Delta V}\sum_{N=1}^{N} d_N \sum_{i=1}^{L} C_N(i)C_{(f,g)}(i)\left\{ u\left[V - V_0 - \frac{\Delta V}{2L}(-L+2i-2)\right] \right. \tag{14}$$

$$\left. - u\left[V - V_0 - \frac{\Delta V}{2L}(-L+2i)\right] \right\}$$

Equations (13) and (14) can be simplified further as follows

$$G1(V) = \frac{P_{sr}}{\Delta V}\sum_{N=1}^{N} d_N \sum_{i=1}^{L} C_N(i)\overline{C}_{(f,g)}(i)\left\{ u\left[\frac{\Delta V}{2L}\right] \right\} \tag{15}$$

$$G2(V) = \frac{P_{sr}}{\Delta V}\sum_{N=1}^{N} d_N \sum_{i=1}^{L} C_N(i)C_{(f,g)}(i)\left\{ u\left[\frac{\Delta V}{2L}\right] \right\} \quad (16)$$

In Eqs. (14) and (15), the data bit of the *N*th user, d_N, carries the value of either "1" or "0." Therefore the photo-detector current can be calculated by integrating process as follows:

$$I_1 = \int_0^{\infty} G_1(v)dv \quad (17)$$

and

$$I_2 = \int_0^{\infty} G_2(v)dv \quad (18)$$

By using the properties of VC code to obtain pure photocurrent after subtract process upon the photo-detectors, Eqs. (17) and (18) become:

$$\mathbf{I}=I_2-I_1= \int_0^{\infty} G_1(v)dv - \int_0^{\infty} G_2(v)dv \quad (19)$$

After integrating and subtraction processes, the photocurrent can be expressed as:

$$\mathbf{I} = \Re \frac{P_{sr}}{L} W \quad (20)$$

$$\Re = \frac{\eta e}{hV_c} \quad (21)$$

Since the noises in photodetector 1 and 2 are independent, the power of noise sources that exist in the photocurrent can be written as [8]:

$$\langle I_{Tot}^2 \rangle = \langle I_{piin}^2 \rangle + \langle I_{sh}^2 \rangle + \langle I_{th}^2 \rangle \quad (22)$$

From Eq. (22):

$$\langle I^2 \rangle = 2eB(I_1 + I_2) + BI_1^2\tau_{c1} + BI_2^2\tau_{c2} + \frac{4K_bT_nB}{R_L} \quad (23)$$

Therefore

$$\langle I^2 \rangle = 2eB\Re\left[\int_0^{\infty} G_1(v)dv + \int_0^{\infty} G_2(v)dv \right] + B\Re^2 \int_0^{\infty} G_1^2(v)dv + B\Re^2 \int_0^{\infty} G_2^2(v)dv + \frac{4K_bT_nB}{R_L} \quad (24)$$

From Eq. (10), when all the users are transmitting bit ''1'' using the average value as $\sum_{N=1}^{N} c_N \approx \frac{NW}{L}$ and the noise power can be written as:

$$\langle I_{Tot}^2 \rangle = 2eB\left[\frac{P_{sr}}{L}((N-1)+W+(N-1)\right] + B\Re^2\left[\frac{P_{sr}^2}{\Delta VL}\cdot\left[\frac{NW}{L}\right].\left[\begin{matrix}(N-1)+W\\+(N-1)\end{matrix}\right]\right] + \frac{4K_bT_nB}{R_L} \quad (25)$$

Noting that the probability of sending bit '1' at any time for each user is a $\frac{1}{2}$ [7-8, 16], then Eq. (25) becomes:

$$\langle I_{Tot}^2 \rangle = \frac{P_{sr} e B \Re}{L}\left[(2N-2)+W\right] + \frac{P_{sr}^2 B \Re^2 NW}{2\Delta V L^2}\left[(2N-2)/(P+R)+W\right] + \frac{4K_b T_n B}{R_L} \quad (26)$$

From Eqs. (20) and (26), the average of SNR is as shown as in Eqs. (27) and (28)

$$\text{SNR} = \frac{(I_2 - I_1)^2}{\langle I_{Tot}^2 \rangle} \quad (27)$$

$$SNR = \frac{\frac{\Re^2 P_{sr}^2 W^2}{L^2}}{\frac{P_{sr} e B \Re}{L}\left[(N-1)+W\right] + \frac{P_{sr}^2 B \Re^2 N}{2\Delta V L^2}\left[W+2(N-1)/P+R\right] + \frac{4KBT_n B}{R_L}} \quad (28)$$

where $\Re$ is the photodiode responsivity. The Bit Error Rate (BER) is computed from the SNR using Gaussian approximation as [7-8, 16].

$$\text{BER} = 0.5 \text{ erfc } \sqrt{SNR/8} \quad (29)$$

For numerical simulations, the following parameters are used: P_{sr}= -10 dBm is the optical received power, ΔV=3.75 THz is the line width of the broad band source, B=311 MHz is the receiver noise-equivalent electrical bandwidth, T_n= 300 K, R_L= 1030 Ω , the bit-rate is at 622 Mb/s, η =0.6 is the photodiode quantum efficiency and λ=1550 nm is the operating wavelength [7-10].

5. Code Evaluation and Comparison

A series of code family with ideal in-phase CC is achieved. For comparison, the properties of the VC, MQC, MDW, MFH and Hadamard are listed in Table 2. It shows that VC codes exist for any positive integer (regardless whether it is even, odd, prime, etc), while MDW exists for even n weights, Hadamard codes exist only when the weight is 2^{m-1} where $m \geq 2$, MQC and MFH exist for a prime number p and a prime power Q given by $Q = p^n$ where n is a positive integer, respectively. The table also shows that the VC codes have an ideal cross correlation while the Hadamard codes have an increasing value of cross correlation as the number of users increased.

The performance of the VC in terms of code length is also compared with that of reported codes. For comparison, the properties of VC, MQC, and MFH are listed in Table 3. Table 3 shows the codes lengths required by MQC (W=6), MFH (W=6) and VC (W=2, P=8, R=1) to support 25 users. From the table we can observe that, VC provides better performance than other codes for same number of users in terms of code length. Long length is a disadvantage since the code is subject to either very wide band source or narrow filter bandwidths are required while short length limits the freedom of code selection. The VC exists for practical code length that is neither too long nor too short.

Table 2. SAC-OCDMA Codes Comparison.

Code family	Existence	Weight	Size	Λ	Code length	SNR
MQC	Primes $p>2$	$p+1$	p^2	1	p^2+p	$\frac{\Delta v(p+1)}{BK[(K-1)/p+p+K]}$ [7,8]
MFH	All GF	$q+1$	q^2	1	q^2+q	$\frac{\Delta v(Q+1)}{BK[(K-1)/Q+Q+K]}$ [7,8]
MDW	Even integer n	n	w/2+1	1	$3n+8/3[\sin(N\pi/3)]^2$	$\frac{2(\frac{w}{4}-1)\Delta v}{BK[(\frac{K}{2}+\frac{w}{4}-2]}$ [9]
Hadamard	$m \geq 2$	2^{m-1}	2^m-1	2^{m-2}	2^m	$\frac{\Delta v}{BK(K+1)}$ [5]
VC	$N>W+1$	Positive integer	Any number of users	1	$(WN+R(W+1-R))/2$	Refer to Eq. (27)

Table 3. Comparison of VC, MQC and MFH for the Same Number of Users, $N = 25$.

Code	Number of users	Weight	λ	Code length
MQC	25	6	1	30
MFH	25	6	1	30
VC	25	2	1	26

6. Results and Discussion

The eye pattern diagrams for VC code for a different fiber links is shown in Fig. 6. The eyes diagram illustrated in Fig. 6 clearly explain that the VC code using a short fiber link (Fig. 6(b)) gives better performance, having a larger eye opening compared to a long fiber link (Fig. 6(a)). The effect of varying the fiber length is related to the power level of the received power. A longer length of fiber has higher insertion loss, thus smaller output power. As a matter of fact, when the fiber length decreases, the data rate should increases to recover a similar degradation of the signal form. Thus, in order to design and optimize link parameters, the maximum fiber length should be defined as short as possible, to obtain high data rate and to achieve a desired system performance. The equivalent simulated BER for VC code for a different fiber links is shown in Fig. 5. In Figs. 6(a) and (b), the estimated BERs for VC are 10^{-29} and 10^{-22} for 25 and 50 km respectively which are satisfactory in practical communication systems.

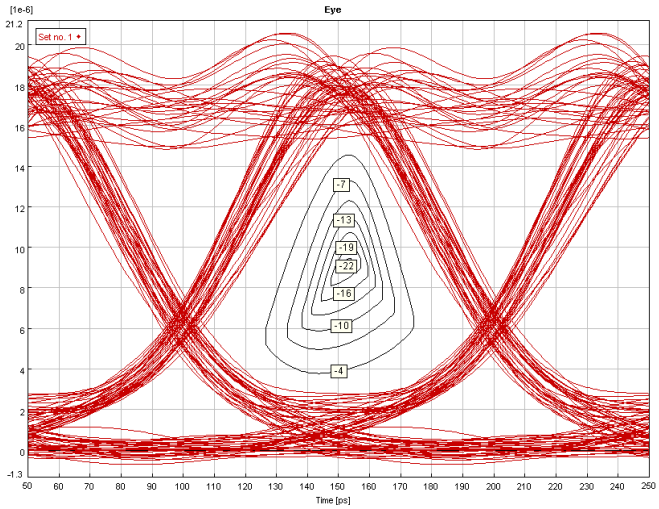

(a)

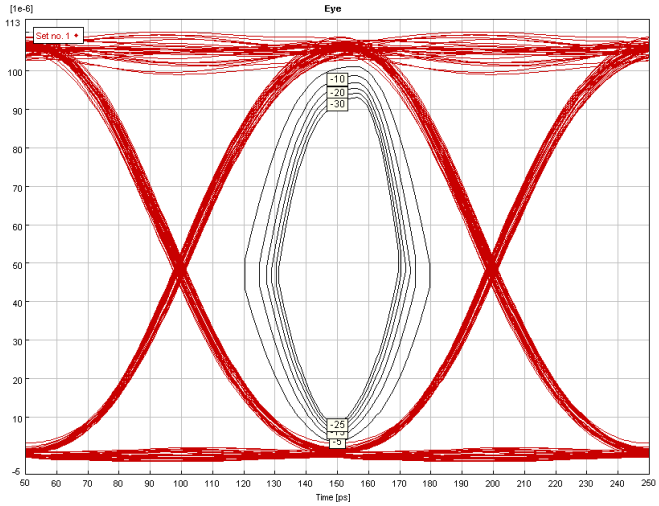

(b)

Fig. 6. Eye Diagram of (a) One of the VC Channels Using a 50 km Fiber Link, (b) One of the VC Channels Using a 25 km Fiber Link, at 10 Gbit/s.

Figure 7 shows the BER variations with the effective power for the VC code when W=4, for a 25 km at 10Gbit/s. It demonstrates the typical linear dependence of the signal power variation due to additive noise and the laser power in dBm. We have found that in order to transmit over a dispersive fiber, a dispersion compensation techniques have to be used. However, the transmission distance remains limited due to the attenuation in the fiber and the noise generation in the detectors.

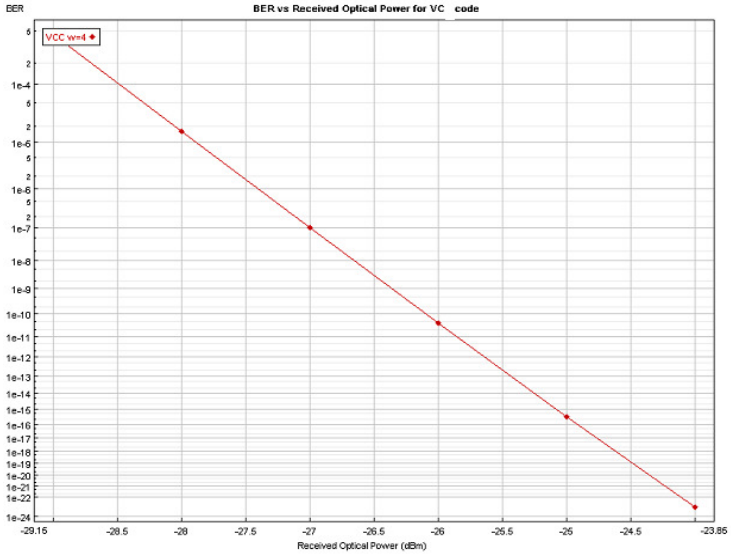

Fig. 7. BER versus Received Power P_{sr} for a 25 km Fiber Link at 10 Gbit/s.

Figure 8 shows the relation between the number of active users and the SNR when the parameters used for the VC, MQC, MFH and Hadamard codes are W=6, 14, 17, 64 respectively while the P=3, R=1 for VC code. In this figure, the effective power from each user is -10dBm taking into account the effects of intensity noise, shot noise and thermal noise. It is shown that the VC code gives much higher SNRs than MQC, MFH, and Hadamard. With a big values of P and R higher SNR can be obtained even for small weight while accommodates high number of active users.

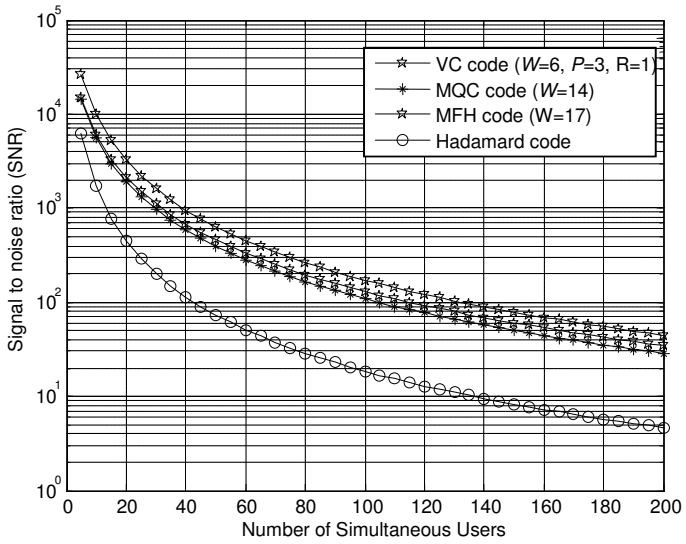

Fig. 8. SNRs versus the Number of Active Users when P_{sr} = - 10 dBm.

In Fig. 9, the BER is plotted against the number of active users when P_{sr} = -10 dBm at 622 Mbit/s. From the figure, we can observe the lower BER of VC code compared with the MQC, MFH and Hadamard codes even though the weight is far less which is 6 in this case. The maximum acceptable BER of 10^{-9} was achieved by the VC code with 120 active users. This is better considering the small value of weight used. This is evident from the fact that VC code has an ideal in-phase cross correlation while Hadamard code has increasing value of cross-correlation as the number of users increase. The calculated BER for VC was achieved for W = 8 while for MFH, MQC and Hadamrad codes were for W = 10, W = 12, and W = 64 respectively.

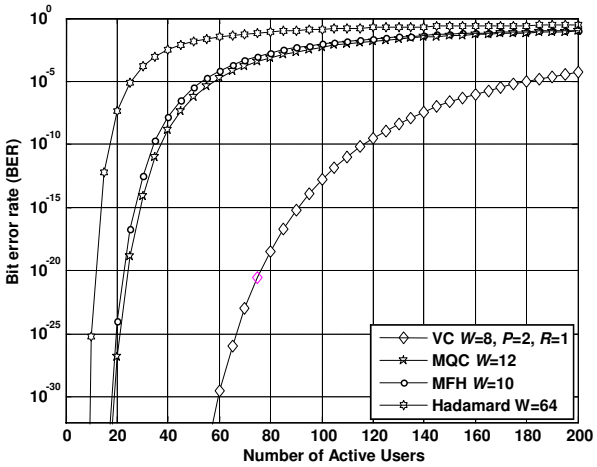

Fig. 9. BERs versus the Number of Active Users for Various Codes Utilizing Spectral Amplitude Coding when P_{sr} = -10 dBm at 622 Mbit/s.

Figure 10 shows the BER variations with the effective power P_{sr} when the number of active users is 30 at a data rate of 2.5 Gb/s for each user, taking into account the effects of the intensity noise, thermal noise and shot noise. VC is adopted with the parameters W=6 and P=4, R=1, while for MQC and MFH the parameters were W=14, W=17, respectively. The figure proves that the efficient source power for the VC is less (-22 dBm) than that for the MQC and MFH codes when the number of active users is the same. When we compare Fig. 7 and Fig. 10, one can see there is contradict between the result obtained from simulation and theoretical study. This is because, firstly in the theory, the effects of attenuation, fiber non-linearity, and insertion loss are not considered. Secondly the number of users in simulation was 2 while in a theoretical was 30.

The computed BER versus channel spacing width is shown in Fig. 11 for a 50 km fiber length. The pulse duration is fixed to T_c = 1/(data rate × code length). As the channel spacing width goes from very narrow to wider, the BER decreases, best performance occurs at a spacing bandwidth between 0.8 (100 GHz) and 1 nm. The reason for the BER increasing after the minimum is that the SNR improvement due to the use of wider optical bandwidth is counteracted by an increased crosstalk/overlapping between adjacent frequency bins that yield MUI. Note that, decreasing channel spacing the effects of four-wave mixing on optical

transmission and in single mode fiber are appeared, this is noticeable as degradation of optical SNR and the system BER performance.

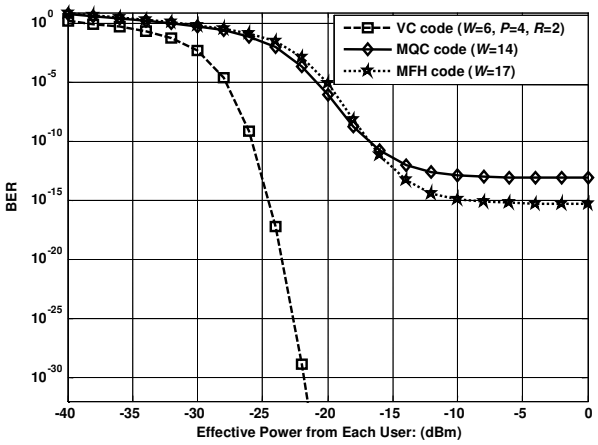

Fig. 10. BERs versus Effective Source Power *Psr* when the Number of Active Users is 30, Taking into Account the Intensity Noise, Shot Noise, and Thermal Noise at the Data Rate 2.5 Gb/s.

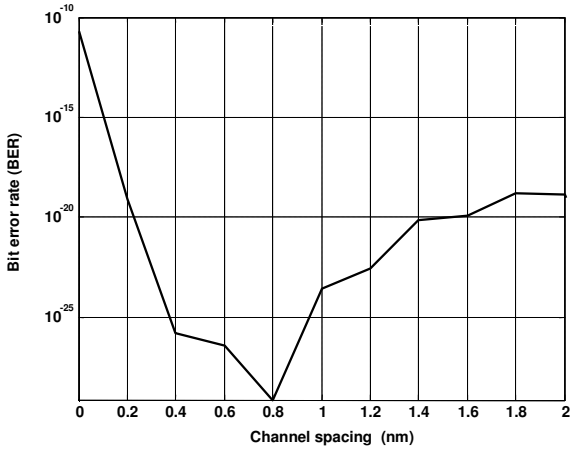

Fig. 11. Variation of BER as a Function of Channel Spacing Width for VC Code when *W*=4 and *N*=2 for a 50 km Fiber Length at 10 Gbit/s.

7. Conclusions

In this paper, we have proposed an efficient method to construct a new code family for the SAC optical CDMA systems with maximum cross-correlation value of 1. The properties of this code family have been discussed and proved using VPI^{TM} simulation software. Structures of both transmitter and receiver for the VC have been verified using FBG groups. The performances of the system were characterized by referring to effective power, SNR and BER, taking into account the effects of the intensity noise, thermal noise and shot noise of both

this system and former systems using MQC and MFH. Furthermore, in comparison with the systems employing MQC and MFH, the proposed system can effectively reduce the power of beating signals sent from other users. From the calculated results, the proposed system outperforms other codes in terms of cardinality and code length. Long length is a disadvantage since the code is subject to either very wide band sources or narrow filter bandwidths are required while short length limits the freedom of code selection. Therefore, there is a tradeoff between the code length and system performance. Our simulation results reveal that, for high data rate the proposed system can accommodated high number of users with low effective power. The advantage of the VC code family can be summarized as follows

- Large flexibility in choosing the number of users than previously reported codes (free cardinality),
- good property in cross-correlation control,
- practical code length, and
- easy to implement using fiber Bragg gratings (FBGs).

Acknowledgment

The authors would like to thank the University Tecknolgi PETRONAS for sponsoring this work under project grant GA.

References

1. Salehi, J.A. (1989). Code division multiple-access techniques in optical fiber network. I. Fundamental principles. *IEEE Transactions on Communications*, 37(8), 824-833.
2. Salehi, J.A.; and Brackett, C.A. (1989). Code division multiple-access techniques in optical fiber networks. II. Systems performance analysis. *IEEE Transactions on Communications*, 37(8), 834-842.
3. Stok, A.; and Sargent, E.H. (2000). Lighting the local area: optical code division multiple access and quality of service provisioning. *IEEE Network*, 14(6), 42-46.
4. Prucnal, P.R.; Santoro, M.A.; and Fan, T.R. (1986). Spread spectrum fiber-optic local area network using optical processing. *Journal of Lightwave Technology*, 4(5), 547-554.
5. Kavehrad, M.; and Zaccarh D. (1995). Optical code-division-multiplexed systems based on spectral encoding of noncoherent sources. *Journal of Lightwave Technology*, 13(3), 534-545.
6. Djordjevic, I.B.; and Vasic, B. (2004). Combinatorial constructions of optical orthogonal codes for OCDMA systems. *IEEE Transactions on Communications*, 21(3), 391-393.
7. Zou, W.; Shalaby, H.M.H.; and Ghafouri-Shiraz H. (2002). Modified quadratic congruence codes for fiber Bragg-Grating-based SAC-OCDMA. *Journal of Lightwave Technology*, 19(9), 1274-1281.
8. Zou, W.; and Ghafouri-Shiraz H. (2002). Unipolar codes for spectral-amplitude-coding optical CDMA systems. *IEEE Transactions on Communications*, 50(8), 1209-1212.

9. Aljunid, S.A.; Ismail, M.; Ramli, A.R.; Ali, B.M.; and Abdullah, M.K. (2004). A new family of optical code sequences for spectral-amplitude-coding optical CDMA systems. *IEEE Photonics Technology Letters,* 16(10), 2383-2385.
10. Abdullah, M.K.; Hasoon, F.N.; Aljunid, S.A.; Shaari, S. (2008). Performance of OCDMA systems with new spectral direct detection (SDD) technique using enhanced double weight (EDW) code. *Optics Communications*, 281(18), 4658-4662.
11. Hasoon, F.N.; Aljunid, S.A.; Abdullah, M.K.; and Shaari, S. (2006). Spectral amplitude coding OCDMA systems using enhanced double weight code. *Journal of Engineering Science and Technology* (*JESTEC*), 1(2), 192-202.
12. Hill, K.O.; and Meltz, G.. (1997). Fiber Bragg grating technology fundamentals and overview. *Journal of Lightwave Technology*, 15(8), 1263-1276.
13. Green, P.E. (1993). *Fiber optic networks*. Prentice Hall.
14. Yang, C.C. (2005). Hybrid wavelength-division multiplexing/spectral-amplitude-coding optical CDMA system. *IEEE Photonics Technology Letters*, 17(6), 1343-1345.
15. Kelley, J.L. (1975). *General topology*. Springer, ISBN 0-387-90125-6.
16. Goodman, J.W. (1985). *Statistical optics*. New York: Wiley-Interscience.